41st Aerospace Sciences Meeting and Exhibit
6-9 January 2003, Reno, Nevada

AIAA 2003-840

Modelling Active Control Technologies using LES

S. Menon*, C. Stone†, H. Feiz‡and J. H. Soo§
School of Aerospace Engineering
Georgia Institute of Technology
Atlanta, Georgia, USA 30332

The next generation gas turbine engines are required to achieve high combustion efficiency and minimal pollutant emission simultaneously over a wide range of operational scenarios. This goal will require new methods that can maximize this performance metric. One approach currently being explored is the use of actively controlled fuel-injectors in order to optimize fuel-air mixing over a wide range of operational conditions. Here, a numerical tool based on Large-Eddy Simulations (LES) is used to model both stable and unstable combustion in premixed and partially-premixed regimes found in typical swirl-stabilized gas-turbine combustor. Two control methods, swirl- and fuel-modulation, are shown to be able to actively suppress thermo-acoustic instabilities. Finally, in order to couple micro-scale actuators within the fuel injectors a new 3D Lattice-Boltzman Equation (LBE) model is developed. Application and validation of the LBE method for various micro-scale jets and synthetic jets is demonstrated. With this development, a methodology that can couple LBE with LES is now operational to finally attempt LES of actively controlled fuel injection in a full-scale gas turbine engine combustor.

1 Introduction

To develop the gas turbine engines of the twenty-first century intelligent optimization of the design and performance of the engine for specific goals (that may or may not be compatible) will be essential. High combustion efficiency and minimal pollutant emission simultaneously over a wide range of operational scenarios is desired but will require new technologies that encompass new hardware and software solutions. Since the physical phenomena of interest are intrinsically linked to the dynamics of the actual process of combustion, i.e., fuel injection, fuel-air mixing, and combustion and heat release, understanding the physics of these processes is critical to developing new methods to achieve hitherto unavailable performance metrics. Current experimental efforts are focussing on demonstrating active control of the combustion process as a means to achieve the aforementioned goal of efficient combustion over a wide range of operating condition. However, the hostile (to non-intrusive measurements) combustion environment makes detailed measurements and parametric evaluation of the performance metrics very difficult, if not impossible. Furthermore, parametric evaluation of design parameters experimentally is economically very expensive and may not be insightful since detailed measurements are difficult.

Therefore, a computational tool that can investigate such complex processes can help supplement experimental verification by providing physical insight into the processes that directly control the combustion processes. Since the physics of processes of interest is time-dependant, a simulation tool that can capture the spatial/temporal evolution can play an important role in the design cycle of future gas turbine engines.

The present effort is directed towards developing and demonstrating advanced computational tools that can be utilized to investigate active control of combustion dynamics in gas turbine engines. To achieve this goal many tools have to be developed and integrated in a seamless simulation tool. Validation of each of the subsets of the final tool is also essential in order to achieve the final goal. A particular goal is to develop a methodology that can be used to investigate combustion process that impact pollutant emission. There is currently a high demand for clean burning combustion devices due to increasingly stringent emission regulations on Oxides of Nitrogen (NO_x), Carbon-Monoxide (CO) and Unburned Hydrocarbons (UHC). The desired emission levels can be ideally achieved by operating in the lean limit. The lower associated combustion temperatures result in the suppression of thermal NO_x pathways. However, as the equivalence ratio (Φ) approaches the *Lean-Blowout* limit (LBO), the sensitivity to small perturbations in fuel concentration, flow velocity, temperature, and pressure increase due to the strong dependence of flame speed on local fuel content. Under certain conditions, these fluctuations can become self exciting, resulting in high-amplitude pressure oscillations. Structural fatigue, increased combustor core noise or possibly even system failure could

*Professor, Associate Fellow, AIAA
†Student Member, AIAA
‡Student Member, AIAA
§Graduate Research Assistant

result if these oscillations are not positively controlled and attenuated.

Therefore, active control is needed to suppress such unwanted instabilities. Many active control techniques are being explored, such as, adaptive fuel modulation, vortex generation, and turbulent boundary layer modulation with synthetic jets. The underlying physical processes behind most of these techniques are not fully understood. Furthermore, experimental evaluation of these configurations are often difficult, if not impossible. As a result, numerical simulations are perhaps, the only feasible alternative to investigate these processes.

Currently, Large-Eddy Simulation (LES) appears to be the only feasible simulation methodology which is capable of capturing unsteady combustion dynamics within the constraint of the computational limits of current technology. In LES, all turbulent length-scales larger then a specified cut-off are resolved in both space and time while modelling is employed for those smaller (referred to as *subgrid-scale* or *sgs*). Larger eddies, those on the order of the geometric length-scale, are highly-anisotropic and their dynamics is strongly dependent on the geometry of the system. Due to the nature of the turbulent energy cascade, energy transfers from large to small scales. To accurately predict the small-scale properties of the flow, the dynamics of the large, energy-containing eddies must therefore be fully captured in the numerical model.

While LES (based on conventional finite-volume solution of the Navier-Stokes equations) is a useful tool when modelling complex turbulent flows (i.e. internal flow in a gas turbine combustor), it is not necessarily computationally efficient for simulating micro-scale devices, such as synthetic micro-jets. Micro devices based on MEMS technology are currently being investigated as efficient devices for active control of the combustion process. The computational cost of simulating the flow within such micro devices while resolving the reacting flow in the combustor is beyond the current processing capability due to the very small time-step that is required to resolve the fastest time scale of the flow (which, in this case, is determined by the flow process within the micro-scale device). This is particularly relevant here since synthetic jets are being evaluated as a device for actively controlling turbulent boundary layers (e.g. flow over a turbine blade) and for enhanced mixing rates in gas turbine engine fuel injectors. To computationally evaluate this type of flow, new techniques have to be developed that can be integrated within the conventional LES methodology.

In the present effort, we are addressing this issue from two directions. The conventional LES methodology is being developed to simulate the turbulent combustion process in the gas turbine combustor, where as, a new simulation methodology based on the Lattice Boltzmann Equation (LBE) method is being developed to simulate micro-scale processes. The LBE model is computationally very efficient and therefore, very high resolution simulations can be performed very quickly. For our application, this allows a high resolution simulation of the small-scale processed without being constrained by the numerical time-step of the LES. The eventual goal is to develop and validate a coupled LES-LBE methodology that can resolve the entire domain of interest (micro to macro). Note that, in principle the LBE approach can also be used to simulate the flow in the gas turbine combustor since the Navier-Stokes equations can be recovered from the Boltzmann equation. However, LBE models have some problems dealing with high speed flow (compressibility and perhaps, even acoustic wave motion effects) and therefore, may not be able to capture acoustic-vortex-heat release coupling. Furthermore, issues related to modelling multi-species finite-rate kinetics within the LBE approach are not yet fully resolved. Therefore, using the conventional finite-volume LES approach for the reacting flow is considered more practical while the LBE will be used primarily to simulate the flow inside the fuel injector (which is at low speed).

Many previous publications have summarized the previous effort in both LES and LBE applications. The effect of swirl on combustion dynamics was studied in detail in the past. Here, the focus will be primarily on studies that addressed some aspects of control of combustion. The results presented here are divided into two parts: (1) the LES studies of swirl and fuel modulation in a gas turbine combustor, and (2) the application of the LBE method to small-scale fuel injectors. While this work has been separated into two distinct divisions, they both share the same final goal: the simulation of active control techniques for the next-generation gas turbine combustion systems.

2 Mathematical Formulation

Here brief descriptions of the mathematical formulation and numerical methods of the LES and LBE modelling techniques.

2.1 Finite-volume LES model

The LES equations of motion are solved on a three dimensional, boundary-conforming grid using an explicit, finite-volume scheme which is fourth-order accurate in space and second-order in time. For brevity, the LES equations and numerical details are withheld but can be found elsewhere.[1–3] No-slip, adiabatic wall conditions conditions are used with non-reflecting inflow/outflow boundary conditions following Poinsot and Lele.[4] Clustering is employed near walls and in shear layer regions to better resolve large scale fluctuations. A one-equation *sgs* kinetic energy model[5] is used to close the momentum and energy equations.

To increase simulation turn-around time, the computational domain is evenly distributed in parallel us-

ing the Message-Passing Interface (MPI) standard. An advantage of the explicit scheme used here is the ease of load balancing since every cell requires the same amount of work resulting in high parallel efficiency. A useful metric for computational cost is the total CPU hours needed for simulation of one flow-through-time (defined as the time needed for a fluid element to pass the length of the combustor (i.e., L/U)). Generally, 7-10 flow-through-times are used requiring 15,000 CPU hours on an IBM Power3-SMP computer.

To simulate the combustion of interest, chemical reactions must be explicitly included in the LES framework. Detailed finite-rate chemical kinetics in LES can be very expensive due to the wide range of chemical time-scales. Fortunately, an alternate, computationally efficient approach exists for premixed and partially-premixed combustion. A premixed flame at moderate turbulent levels can be modelled as a thin surface which is convected and contorted by the local velocity fluctuations. This assumption is valid so long as the flame thickness (δ) is much smaller than η (the turbulent micro-scale) and the burning time-scale is small compared to that of the turbulence. Under these assumptions, the flame remains locally laminar and its burning velocity (directed normal to the surface) is balanced by the local flow. Extensive literature exists on such flame surface models (also known as *flamelet* models), see Peters[6] for more details. As opposed to directly solving a set of N chemical reactions (and N additional conservation equations which are generally quite stiff), premixed *flamelet* models require the solution of only a single scalar field. Obviously this can reduce the computational expense. *Flamelet* models, however, cannot directly predict pollutant emissions or flame extinction since no chemistry is involved; but, they do provide accurate prediction of unsteady heat release and flame-turbulence interactions. Therefore, this flamelet model is used to study combustion dynamics which is interest here.

Following Williams[7] and Kerstein *et al.*,[8] a model equation that describes the convection and propagation of a thin, laminar flame is the G-equation. In LES, the G-equation[9] can be written as:

$$\frac{\partial \overline{\rho}\widetilde{G}}{\partial t} + \nabla \cdot \overline{\rho}\tilde{u}\widetilde{G} = -S^{sgs} - \nabla \cdot G^{sgs}. \qquad (1)$$

where $\widetilde{G}$ is a scalar variable defining the flame location and S_L is the laminar burning velocity of the flame (flame speed). The scalar field $\widetilde{G}$ is defined in the region [0,1] in which the unburnt products are assigned $\widetilde{G} = 1$ and hot, reacted gases are $\widetilde{G} = 0$. The flame surface is defined as an iso-scalar surface, G_0 ($0 < G_0 < 1$). Essentially, this models a level-surface, at $\widetilde{G} = G_0$, being convected by the local flow-field and propagating at S_L. All chemical and diffusive processes are implicitly included in S_L and, therefore, no specific species transport needs to be modelled. The two sub-grid terms, S^{sgs} and G^{sgs}, are, respectively, the filtered source and the unresolved transport. Details on there respective closure may be found elsewhere.[10]

In order to account for local variations in the local fuel composition (i.e., partially-premixed combustion regime), the G-equation must be augmented by a second scalar equation tracking the local mixture fraction, Z. This equation takes following form in LES:

$$\frac{\partial \overline{\rho}\widetilde{Z}}{\partial t} + \nabla \cdot [\overline{\rho}\tilde{u}\widetilde{Z} - \rho D \nabla \widetilde{Z}] = -\nabla \cdot Z^{sgs}. \qquad (2)$$

where Z^{sgs} is closed with a common gradient diffusion model. A benefit of this model this the lack of reaction source terms in Eqn. 2 making this model inexpensive.

For uniform equivalence ratio, heat-release is introduced into the systems by coupling G to the super-grid internal energy,

$$E_i = C_v\ T + C_p\ (T_f - T_0)\ \widetilde{G}, \qquad (3)$$

where T_f and T_0 are the temperatures of the products and reactants, respectively. For non-uniform equivalence ratio, Eqs. 1 and 3 must be adjusted. This case, the value of S_L and T_f are no longer constant but are functions of $\widetilde{Z}$. The functional dependency can be seen in Fig. 1 where both S_L and T_f have been plotted against Z. These results where obtained from the CHEMKIN software package.[11,12] In their modified forms, S_L and T_f in Eqs. 1 and 3, respectively are replaced by $S_L(Z)$ and $T_f(Z)$. The closure of the turbulent burning rate is not changed for this study which limits the current model to only mild or large-scale fluctuations in the local mixture fraction and that the mixture remain lean (i.e., $\Phi < 1$). However, for the present study, which is focused on large-scale temporal/spatial variations in Φ, this should not be a major issue.

2.2 The lattice boltzmann equation LES model

The difference between LBE and Navier-Stokes equation methods is that the microscopic particle distribution (analogous to the particle distribution function in kinetic theory) of the fluid is solved instead of the macroscopic properties of the fluid. The evolution of the distribution function f_α is govern by:

$$f_\alpha(\mathbf{x} + \mathbf{e}_\alpha\delta, t + \delta) - f_\alpha(\mathbf{x}, t)$$
$$= \frac{1}{\tau}[f_\alpha^{eq}(\mathbf{x}, t) - f_\alpha(\mathbf{x}, t)], \quad \alpha = 0, 1, \cdots, 18, \qquad (4)$$

where τ is the relaxation time, f_α^{eq} is the equilibrium distribution function, e_α is the particle speed in α direction and the characteristic speed is $c = \mathbf{e}_\alpha\delta/\delta = |\mathbf{e}_\alpha|$. Rest particles of type 0 with $e_0 = 0$ are also allowed. Note that the time step and the lattice spacing each have equal spacing of unity. Thus, $\delta = 1$.

The 19-bit velocity field is given as:

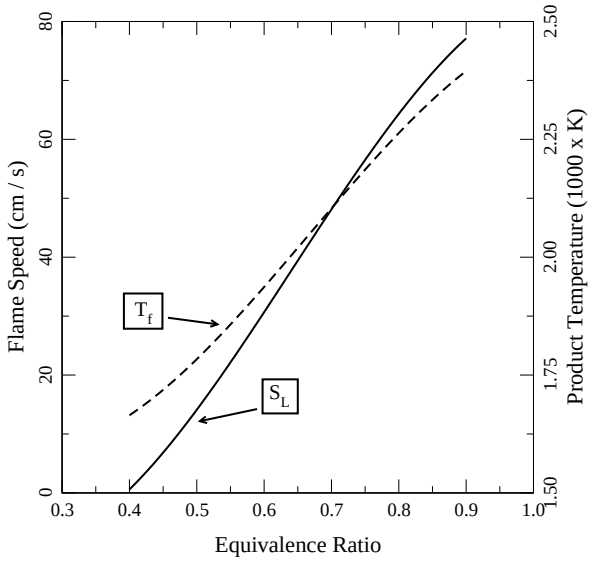

Fig. 1 Flame speed (S_L) and product temperature (T_f) dependence on mixture fraction/equivalence ratio (Z/Φ). Solid and dashed line show S_L and T_f relationships, respectively.

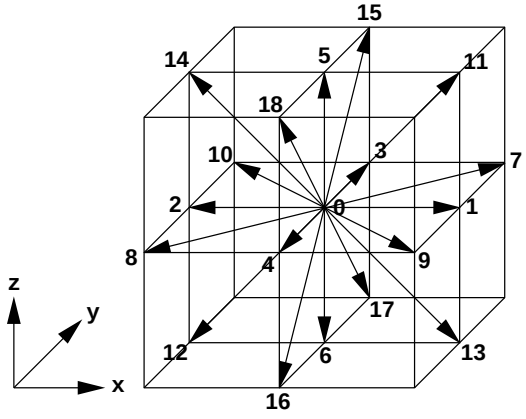

Fig. 2 Link vectors of f_α.

$$\mathbf{e}_\alpha = \begin{cases} (0,0,0) \\ ((\pm1,0,0),(0,\pm1,0),(0,0,\pm1))c \\ ((\pm1,\pm1,0),(0,\pm1,\pm1),(\pm1,0,\pm1))\sqrt{2}c \end{cases} \tag{5}$$

corresponding to the link vectors α shown in Figure 2.

f_α^{eq} is given by the following form:

$$f_\alpha^{eq} = w_\alpha \rho[1 + \frac{3(\mathbf{e}_\alpha \cdot \mathbf{u})}{c^2} + \frac{9}{2}\frac{(\mathbf{e}_\alpha \cdot \mathbf{u})^2}{c^4} - \frac{3}{2}\frac{\mathbf{u}^2}{c^2}], \tag{6}$$

where

$$w_\alpha = \begin{cases} \frac{1}{3} & \alpha = 0 \\ \frac{1}{18} & \alpha = 1,2,\cdots,6 \quad \text{class I links} \\ \frac{1}{36} & \alpha = 7,8,\cdots,18 \quad \text{class II links} \end{cases}$$

The macroscopic properties of the flow field can be obtained by integrating the distribution functions over the velocity space:

$$\rho = \sum_\alpha f_\alpha \tag{7}$$

$$\rho\mathbf{u} = \sum_\alpha \mathbf{e}_\alpha f_\alpha, \qquad \alpha = 0,1,...,18. \tag{8}$$

where ρ is the density and $\mathbf{u}$ is the velocity.

The Smagorinsky sub-grid eddy viscosity model is used in the current simulations. In this method, the macroscopic effects of the sub-grid stresses on the resolved scales are modelled using an eddy viscosity, ν_τ, defined as:

$$\nu_\tau = C_\nu \Delta^2 S. \tag{9}$$

Here, C_ν is the Smagorinsky constant, $\Delta = (\Delta_x\Delta_y\Delta_z)^{\frac{1}{3}}$ is the associated length scale derived from the local volume of the lattice and $S = (2\overline{S_{ij}}\ \overline{S_{ij}})^{\frac{1}{2}}$ is the characteristic filtered rate of strain. The Smagorinsky constant is determined using the localized dynamic model (LDM),[13] which is formulated based on the assumption of scale similarity in the inertial sub-range. The computed eddy viscosity is added to the kinematic viscosity so that the collision relaxation time, which represents the microscopic level counterpart of the viscosity, is allowed to adjust locally.

The boundary conditions used are similar to those initially proposed for the d2q7 model[14] (d denotes the dimension and q the number of links) and adapted to the d3q15 and d3q18 models.[15] At the end of particle streaming, the inward pointing links at the boundary are not defined while the outward pointing ones and those which lie parallel to the boundary surface are known. The general approach in computing these unknowns populations is by first equating populations of the inward and outward pointing links (i.e. bounce-back), thus the density ρ is defined and the normal momentum component neutralized at this node. The tangential momentum of the parallel links is then redistributed to the inward pointing ones which have a tangential component (class II links) to yield zero tangential momentum. To enforce a finite normal velocity at this node, particle distribution is added to the incoming normal class I link.

Similarly, new sets of boundary conditions have to be developed for various physical boundaries of the flow. Boundary conditions for convex and concave corners and edges have been developed and verified in the present effort.

3 LES Results and Discussion

In this section, the suppression of combustion instabilities in a swirl-stabilized dump combustor employing two different (open-loop) control techniques is presented. These two techniques are (1) primary fuel modulation and (2) inlet swirl modulation. The first method, fuel modulation, requires the use of the

partially-premixed combustion model previously mentioned in order to simulate the spatial and temporal variations in the local fuel concentration.

The dump combustor simulated here consists of a straight inlet duct expanding suddenly into the larger combustion zone. The expansion area ratio is 10.25. The inlet and combustor lengths are 1.25 and 5.5 D_i, respectively, where D_i is the inlet diameter. A swirling velocity field (with a 7% Gaussian random field) is specified at the inlet. The inlet velocity profiles are taken from experimental data.[16] For different levels of swirl, the azimuthal velocity is adjusted while the axial profile is held fixed. The mean inlet mass-flow-rate ($\dot{m}$), temperature, and pressure are 0.435 kg/s, 673 K, and 1195 kPa, respectively. The Reynolds number based on the inlet center-line axial velocity and inlet diameter is 527,000. A grid of 181 × 73 × 81 (axial, radial, azimuthal directions, respectively) is used with clustering in regions of high shear. A convergence is placed at the exist to accelerate the product gases for numerical stability at the outflow. In real combustors, there is typically a throat (that may or may not be choked) at the outflow plane. The present study employs a un-choked exit that is similar to some experimental (laboratory-scale) setups. Both un-choked and choked exit planes reflect a portion of the acoustic energy that may or may not play a role in creating thermo-acoustic instabilities.

3.1 Swirl modulation

A simulation has been conducted which looks at the combustion response to variations in inlet swirl (parameterized by the swirl number S). As was previously reported by Stone and Menon,[3] p' is strongly dependent upon the magnitude of S.

Starting from a low value (below the critical value at which *Vortex-Breakdown* occurs), S was gradually increased from 0.56 to 1.12. The rate of increase was slow enough to allow 15 p' cycles so that transients, delay times and possible hysteresis effects can more clearly be observed. The resulting fluctuating mass-flow-rate, $\dot{m}'$, and pressure time histories, along with the time-varying S, are shown in Fig. 3 ($\dot{m}'$ is measured near the exit of the inlet pipe). Prior to changes in S, the rms $\dot{m}'$ is approximately 60% which is consistent with the previously reported u' values through the inlet.[3] After a convective and response time-delay of approximately 6 ms (18 p' cycles), the rms $\dot{m}'$ drops exponentially to less then 5%. After removing the inlet convection time (L_i/U_0), which is 1.5 p' cycles, the overall response time is approximately 15 oscillations. The attenuated $\dot{m}'$ causes a reduction in the longitudinal flame oscillations. In a similar fashion, p' (Fig. 3(b)) approaches an much reduced value after approximately the same time-delay. The overall pressure instability was attenuated by 6 dB during the swirl modulation. For further details, refer to the previous studies on swirl modulation.[17,18]

3.2 Fuel modulation

The current application of the *partially-premixed* model is intended to simulate control of combustion instabilities through primary/secondary fuel modulation. Altering of the upstream equivalent ratio (Φ) can result in changes in the self-excited pressure oscillations.[3] In the current study, the upstream bulk Φ is altered through time to mimic the pulsation of primary fuel flow-rate. During this simulation, the inlet Φ is dropped from an elevated value of 0.62 down to 0.52. Previous studies[19] have shown that at higher equivalence ratios, the amplitude of p' is reduced.

Shown in Fig. 4 is the p' time trace and the analogous imposed inlet Φ. When Φ is elevated at 0.62, the peak-to-peak pressure fluctuations are within +/- 2% and the p' $rms \approx 1.0$. However, once Φ is dropped to 0.52, the peak-to-peak dramatically increases with a subsequent rms increase. Of importance to active control system designers is the time delay or response time. In this situation, the response time is effected by both convection (i.e., the time to travel from the inlet to the flame region) and an acoustic time (i.e., the time for a wave to transfers the combustor). In this case, the response time, measured from the time at which Φ has dropped to its lowest value, is approximately 1.2 ms or 3.5 cycles if non-dimensionalized by the peak frequency. Based on the inlet mass flow rate and inlet length, the convective time is approximately 1/3 ms and is the same for resonant acoustic time. As can be seen, once the changes in Φ have reached the reaction zone, the acoustics respond quickly. Compared to the 15 cycles required by the swirl-modulation control, this response time is much shorter. Further details on *partially-premixed* combustion and active-control can be found in the literature.[10]

4 LBE Simulations of Micro-Scale Devices

The used of the LBE method has been extended to three different jet phenomena: synthetic, square and square jets in cross-flow. All three flows are of interest for turbulent boundary layer control and enhanced fuel/air mixing. A key approach used here is to solve the flow inside the jet as well so the conditions at the jet exit is not specified but naturally evolves under the upstream conditions. This is also critical for the simulation of micro-scale jet devices since the flow at the exit is not necessarily choked and there is significant interactions between the flow inside fuel injectors and external flow. In fact, past studies in certain conditions in gas turbines, fuel line oscillations couple with combustion dynamics inside the combustor and may play a major role in combustion instability. Active control of the fuel injectors may therefore, be a means to eliminate this type of coupling.

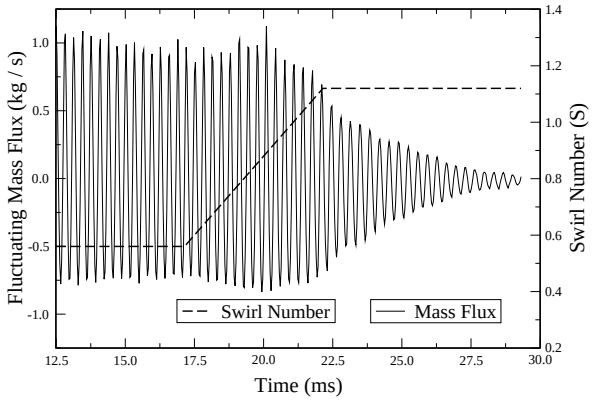

a) $\dot{m}'$

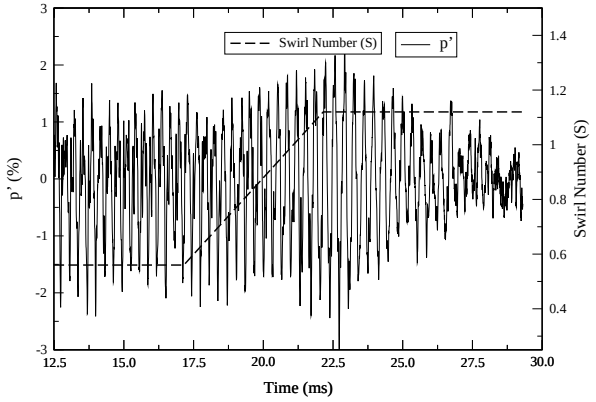

b) p'

Fig. 3 Fluctuating (a) mass-flow-rate (kg/s), $\dot{m}'$, and (b) pressure, p', during inlet swirl number modulation.

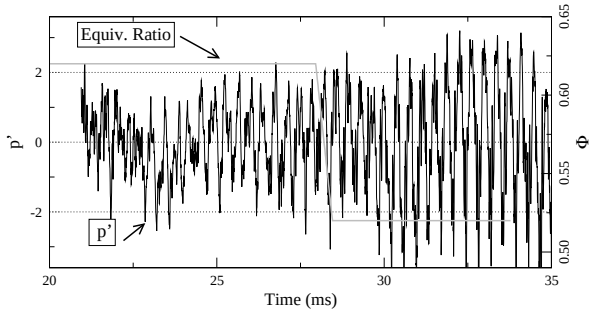

a) $p'(t)$

Fig. 4 Fluctuating pressure (p') and equivalence ratio (Φ) through time for temporal Φ variation simulation. Φ is shown with symbols while p' is shown with a black line.

4.1 Synthetic jet

The geometry for the baseline synthetic jet case with rectangular orifice aspect ratio of 15 (denoted as SN1) is shown in Fig. 5. For the purpose of model validation against experimental data, another test case (SN2) which has an extended orifice aspect ratio of 25 is also used. For the present paper only representative results are shown for the SN1 test case. More detailed analysis and comparisons will be reported in the near future.

The accuracy of the symmetric boundary condition and the grid independence of the solution are first evaluated. Comparison between a full domain and a quarter domain simulation in Fig. 6(a) shows excellent agreement in the near-field region of the orifice. Grid independence is shown in Fig. 6(b) where adequate convergence with the present resolution is achieved. A grid resolution of $150 \times 120 \times 68$, $32 \times 120 \times 13$ and $180 \times 240 \times 100$ (medium case in Fig. 6(b)) grid points are used for the cavity, nozzle and discharge domains, respectively, has been chosen for subsequent studies.

SN2 has been validated against experimental data from Smith and Glezer[20] and compared with the numerical predictions of Rizetta et al.[21] For the experiments, the Smith and Glezer employed an orifice aspect ratio of 150 and measurements were taken at the orifice mid-span to recover a quasi 2D system. The mean stream-wise velocity profiles of the mid-span cross section for SN2 non-dimensionalized with the the usual similarity coordinates of conventional 2D jets is shown in Fig. 7. The figure shows that the mean jet stream becomes self-similar only for a short downstream distance. For SN2, this region is approximately $8.8 < z/h < 9.8$. With increasing downstream distance, although the center region remains fairly self-similar, the agreement at the outer shear region deteriorates considerably which is related to 3D instabilities.

Fig. 8 suggests that the primary vortex structure breaks down rapidly in the experiment due to the development of secondary vortical rib-like structures about the core of the primary vortex.

The deformation of non-circular vortex structures results in increased mass entrainment through the axis-switching of the vortex structure. Through the manipulation of this process, it is believed that the fuel-air mixing in a combustor can be enhanced due to the augmentation of cross-stream fluxes which brings a larger volume of fuel and air into contact with each other.

The axis-switching of the structure of SN1 is shown in Fig. 10. The formation and evolution of the structures show two distinct difference from typical simulations of isolated rectangular vortex structure[22] that employ an analytic velocity boundary in place of the cavity and the nozzle: (1) the emerging structure is not nominally planar, and (2) the span-wise portions

of the structure is quite distinct from the long flat portions. More detailed analysis and parametric studies will be reported soon.

4.2 Square jet

A square 'orifice' jet perturbed at its preferred jet mode corresponding to Strouhal number of 0.49 is simulated. The dimensions of the simulated case is shown in Fig. 11 and are similar to the geometry of the experimental jet facility whose results are compared with[23] except for the fact that the pipe cross section for which the jet originates from is circular in the experiments (with the reference diameter D in the figure) whereas it is a square in the present simulation. The equivalent diameter used in the present study is however matched to yield actual cross sectional area. Again, the full domain is simulated and forcing is applied at the velocity boundary and therefore, the orifice exit velocity profile is acquired and not assumed. The large-scale structures are resolved and the small-scales modelled in the form of an eddy viscosity based on the localized dynamic model.[13] The velocity fluctuation at the pipe inflow is adjusted to match the ratio of the root-mean-square (RMS) level of the centerline stream-wise velocity fluctuations, the centerline jet velocity $w_o'/\bar{W} = 0.1$, the jet Reynolds number $Re = 9300$ based on $\bar{W}$ and the equivalent diameter D_e of the orifice at the orifice exit plane of the experiment denoted as OU2 in his paper. The acquired parameters for the simulation are $w_o'/\bar{W} = 0.094$ and $Re = 9479$. The computational domain is divided into three sub-domains and $150 \times 150 \times 74$, $68 \times 68 \times 6$ and $200 \times 200 \times 100$ grid points are used for the pipe, nozzle and outflow domains, respectively.

The visualization of the evolution of the coherent structures is shown in Fig. 12. In addition to the axis-switching square structures, braid vortices are formed due to the redistribution and stretching of the stream-wise vorticity between adjacent square structures.[22] Due to the deformation of these coherent structures, the jet half-widths across the mid-span plane and the diagonal plane undergo different spreading and contraction rates. Fig. 13 compares the jet half-widths of the mean stream-wise velocity with the experiment. The profiles near the orifice show reasonable agreement with the global trends although two primary general differences are observed: (1) the spreading rates are generally faster for the experiment, and (2) axis crossover of the mean jet occurs more frequently and more rapidly in the simulation. It has been observed that in general, the evolution of external flow-field is very sensitive to both inflow conditions and orifice irregularities. Inflow turbulence and surface irregularities can trigger shear layer instability that can enhance the breakdown of large-scale structures to small-scale 3D turbulence. Breakdown to turbulence may also be enhanced by the axis switching process. Current effort is focussed on a more in-depth evaluation of these issues.

Interestingly, the axis crossover of the jet occurs faster than the all the simulations of Grinstein[23] where an analytic velocity boundary is used in place of the pipe and nozzle (the author showed at most two crossovers within $0 < z/D_e < 3$ compared to two within $0 < z/D_e < 2$ for the present case). Also, the profiles within $0 < z/D_e < 1$ are generally flat in his simulation, whereas for the present case the axis switching mechanism is already initiated at this location. More detail have been reported elsewhere.[24]

5 Conclusion

Various simulations of active control technologies have either directly or indirectly shown. Through the use of Large-Eddy Simulation (LES), unstable premixed and *partially-premixed* combustion has been modelled and two methods for actively suppressing these instabilities has been investigated. It is shown that both swirl modulation and adaptive fuel injection can be effective in reducing the magnitude of combustion instabilities. Efforts are currently under way to extend the present combustion model to prediction of pollutant formation in an unstable combustion environment. Although the current studies have been focussed on open-loop control issues the eventual goal is to do active feedback control of fuel-air mixing. Finally, in order to carry out active control, the flow field inside and caused by the actuator has to be simulated as well. Here, a new 3D highly-parallel Lattice-Boltzman (LBE) model has been developed for both DNS and LES and applied to flows of relevance. The LBE approach has been validate by applying it to simulate synthetic and square jets. Future studies will integrate this LBE-LES approach within the full Navier-Stokes equation based reacting LES solver for application to a simulation of actively controlled fuel injector in a gas turbine combustor.

6 Acknowledgments

This work is financially supported in part by the Army Research Office (ARO) and General Electric Power Systems. The High Performance Computing (HPC) resources provided by the Department of Defense (DOD) Major Shared Resources Centers (MSRC) at Naval Oceanographic Office (NAVOCEANO), Army Research Laboratory (ARL), and Army Engineering Research and Development Center (ERDC) under the Army Research Office (ARO) Grand Challenge Project.

References

[1] Kim, W.-W., Menon, S., and Mongia, H. C., "Large eddy simulations of a gas turbine combustor flow," *Combustion Science and Technology*, Vol. 143, 1999, pp. 25–62.

[2] Kim, W.-W. and Menon, S., "Numerical modeling of turbulent premixed flames in the thin-reaction-zones regime," *Combustion Science and Technology*, Vol. 160, 2000, pp. 110–150.

[3] Stone, C. and Menon, S., "Parallel Simulations of Swirling Turbulent Flames," *Journal of Supercomputing*, Vol. 22, 2002, pp. 7–28.

[4] Poinsot, T. and Lele, S., "Boundary conditions for direct simulations of compressible viscous flow," *Journal of Computational Physics*, Vol. 101, 1992, pp. 104–129.

[5] Schumann, U., "Subgrid scale model for finite difference simulations of turbulent flows in plance channels and annuli," *Journal of Computational Physics*, Vol. 18, 1975, pp. 376–404.

[6] Peters, N., *Turbulent Combustion*, Cambridge University Press, 2000.

[7] Williams, F. A., *Combustion Theory*, Benjamin/Cummins, 1985.

[8] Kerstein, A. R., Ashurst, W. T., and Williams, F. A., "The field equation for interface propagation in an unsteady homogeneous flow field," *Physical Review A*, Vol. 37, 1988, pp. 2728–2731.

[9] Smith, T. M. and Menon, S., "The structure of premixed flames in a spatially evolving turbulent flow," *Combustion Science and Technology*, Vol. 119, 1996, pp. 77–106.

[10] Stone, C. and Menon, S., "LES of Partially-Premixed Unsteady Combustion," *AIAA Paper 2003–0310*, 2003.

[11] Kee, R. J., Grcar, J. F., Smooke, M. D., and Miller, J. A., "A Fortran program for modeling steady laminar one-dimensional premixed flames," *Sandia Report SAND85-8240, Sandia National Labs., Livermore, CA.*, 1993.

[12] Kee, R. J., Rupley, F. M., and Miller, J. A., "Chemkin-II: A Fortran chemical kinetics package for the analysis of gas phase chemical kinetics," *Sandia Report SAND89-8009B, Sandia National Labs., Livermore, CA.*, 1993.

[13] Kim, W.-W. and Menon, S., "A new dynamic one-equation subgrid model for large-eddy simulations," *AIAA Paper 95-0356*, 1995.

[14] Noble, D. R., Chen, S., Georgiadis, J. G., and Buckius, R. O., "A consistent hydrodynamic boundary condition for the lattice Boltzmann mehtod," *Physics of Fluids*, Vol. 7, No. 1, 1995, pp. 203–209.

[15] Maier, R. S., Bernard, R. S., and Grunau, D. W., "Boundary conditions for the lattice Boltzmann method," *Physics of Fluids*, Vol. 8, No. 7, 1996, pp. 1788–1801.

[16] Joshi, N. D., Mongia, H. C., Leonard, G., Stegmaier, J. W., and Vickers, E. C., "Dry Low Emissions Combustor Development," *ASME Paper 98GT-310*, 1998.

[17] Stone, C. and Menon, S., "Adaptive Swirl Control of Combustion Dynamics in Gas Turbine Combustors," *Proceedings of the 29th International Symposium on Combustion (to appear)*, 2002.

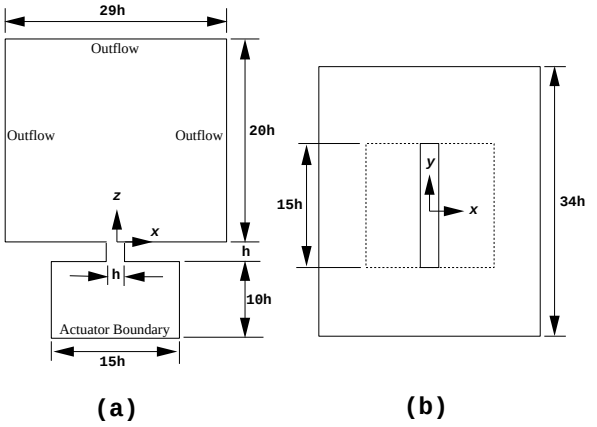

Fig. 5 Synthetic jet (SN1) computational domain: (a) side view, (b) top view.

[18] Stone, C. and Menon, S., "Open-Loop Control of Combustion Instabilities in Gas Turbine Combustors," *Proceedings of the 5th International Symposium on Engineering Turbulence Modelling and Measurements, ETMM5*, 2002, pp. 895–905.

[19] Stone, C. and Menon, S., "Combustion Instabilities in Swirling Flows," *AIAA Paper 2001–3846*, 2001.

[20] Smith, B. L. and Glezer, A., "The formation and evolution of synthetic jets," *Physics of Fluids*, Vol. 10, No. 9, 1998, pp. 2281–2297.

[21] Rizetta, D., Visbal, M., and Stanek, M., "Numerical investigation of synthetic-jet flowfields," *AIAA Journal*, Vol. 37, No. 8, 1999, pp. 919–927.

[22] Grinstein, F. F., "Vortex dynamics and entrainment in rectangular free jets," *Journal of Fluid Mechanics*, Vol. 437, 2001, pp. 69–101.

[23] Grinstein, F. F., Gutmark, E., and Parr, T., "Near field dynamics of subsonic free square jets. A computational and experimental study," *Physics of Fluids*, Vol. 7, No. 6, 1995, pp. 1483–1497.

[24] Feiz, H., Soo, J.-H., and Menon, S., "LES of turbulent jets using the lattice boltzmann approach," *AIAA Paper 2003-0780*, 2003.

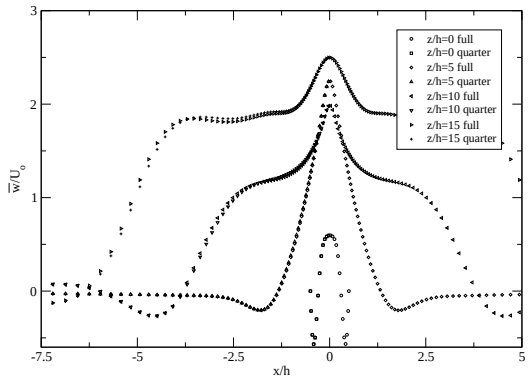

a)

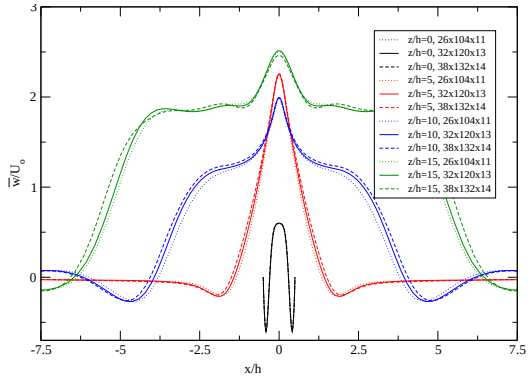

b)

Fig. 6 (a) Comparison of mid-span stream-wise velocity at the orifice and various stream-wise locations between a full and quarter domain. (b) Solution from three different resolutions. Legend represents number of grid points at the nozzle.

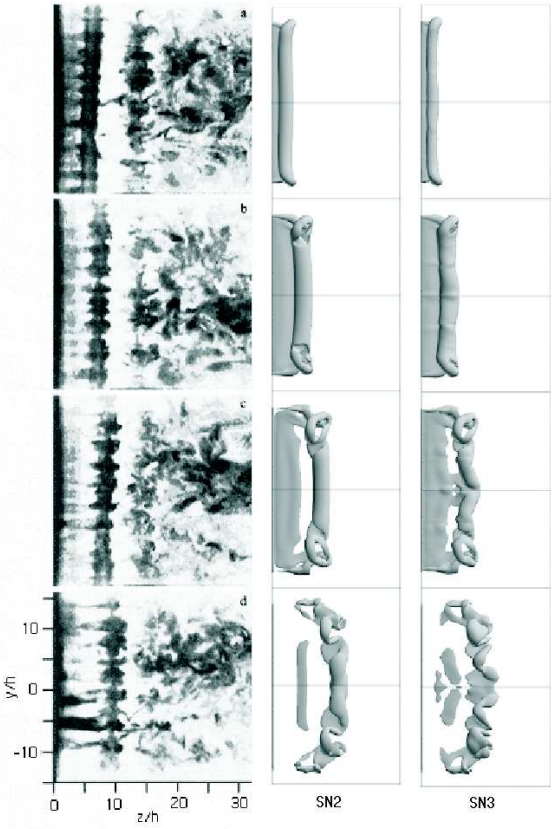

Fig. 8 Qualitative comparison of the vortical structures with experiment[20] at $t/T = 0.5, 0.625, 0.75, 0.875$ with T the actuator period and $t/T = 0.0$ is the instance at which the forward motion of the actuator diaphragm starts. Vorticity magnitude for the simulated cases are held constant at $0.063\omega_{max}$ for SN1 at $t/T = 0.5$.

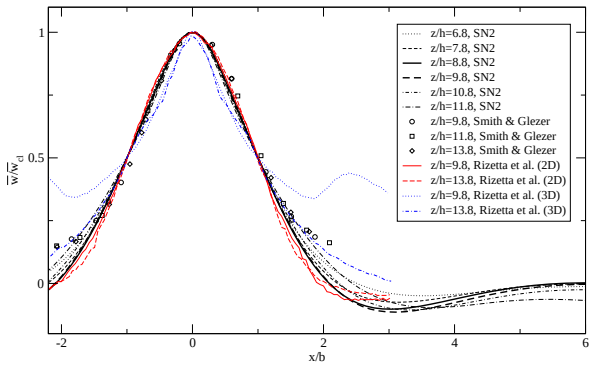

Fig. 7 Mean stream-wise velocity across the orifice mid-span at various downstream locations normalized using similarity coordinates compared to experimental[20] and numerical results.[21] Here, b is the jet half-width and $\bar{w}_{cl}$ is the mean centerline velocity.

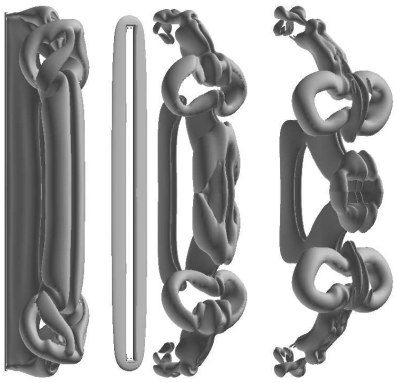

Fig. 9 The evolution of the vortex structure in terms of the iso-surfaces of vorticity magnitude. The magnitude is held constant for each time level: **a)** $\Omega = 0.14\Omega_{max,SN2}$, **b)** $\Omega = 0.12\Omega_{max,SN2}$, **c)** $\Omega = 0.10\Omega_{max,SN2}$, **d)** $\Omega = 0.060\Omega_{max,SN2}$, where $\Omega_{max,SN2}$ is at $t^\star/T = 0.5$.

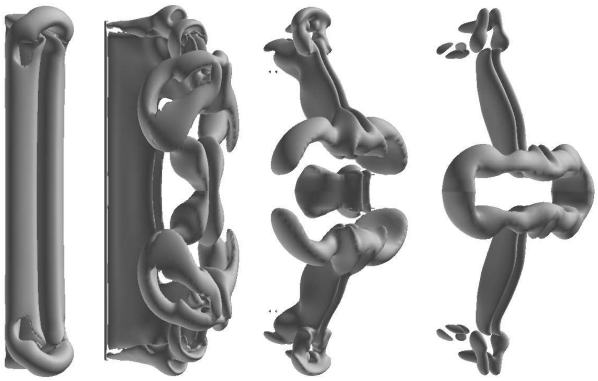

a) b) c) d)

Fig. 10 Evolution of the vortex structure of SN1 at regular time intervals of $t^\star/T = 0.25$ starting at $t^\star/T = 0.25$ in terms of the iso-surfaces of the vorticity magnitude: a) $\Omega = 0.11\Omega_{max}$, b) $\Omega = 0.084\Omega_{max}$, c) $\Omega = 0.043\Omega_{max}$, d) $\Omega = 0.030\Omega_{max}$, where Ω_{max} is with respect to the first sequence.

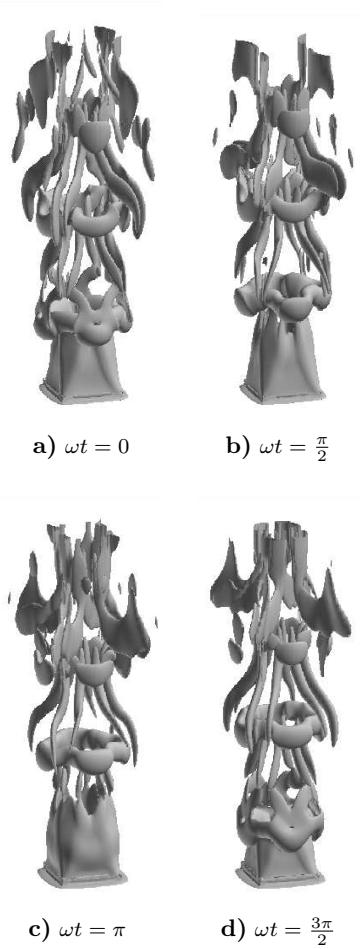

a) $\omega t = 0$ b) $\omega t = \frac{\pi}{2}$

c) $\omega t = \pi$ d) $\omega t = \frac{3\pi}{2}$

Fig. 12 Iso-surfaces of vorticity magnitude over a forcing cycle for the square jet.

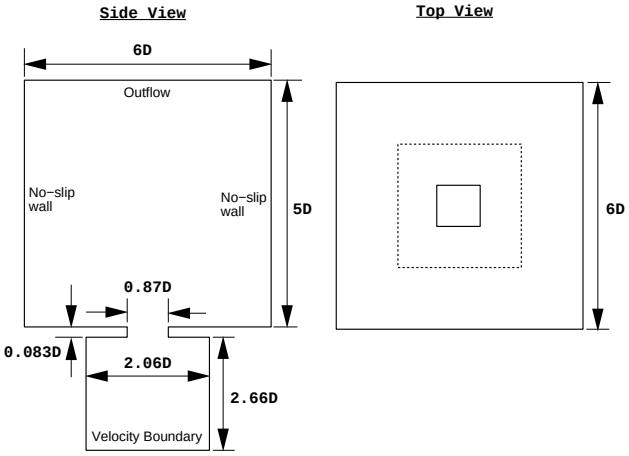

Fig. 11 Square jet geometry.

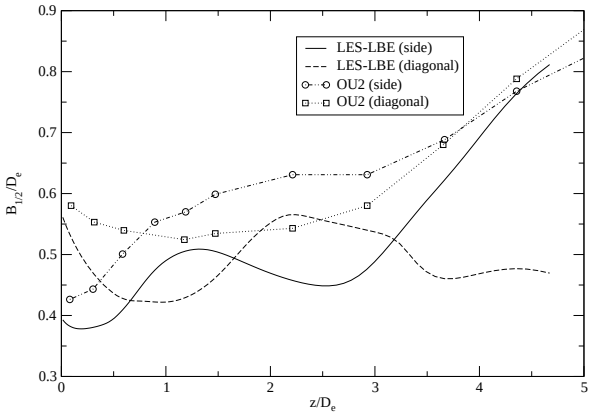

Fig. 13 Mid-span and diagonal plane jet half-width spreading rates for the square jet.